
Elixir: Train a Large Language Model on a Small GPU Cluster

Haichen Huang
HPC-AI Technology Inc.
hhc@hpcaitech.com

Jiarui Fang *
HPC-AI Technology Inc.
fangjr@hpcaitech.com

Hongxin Liu
HPC-AI Technology Inc.
liuhongxin@hpcaitech.com

Shengui Li
HPC-AI Technology Inc.
lisg@hpcaitech.com

Yang You †
National University of Singapore
you@comp.nus.edu.sg

Abstract

In recent years, large language models have achieved great success due to their unprecedented size. However, training these models poses a challenge for most researchers as it requires a substantial number of GPUs. To reduce GPU memory usage, memory partitioning and memory offloading have been proposed. These approaches eliminate memory redundancies and offload memory usage to the CPU and NVMe memory, respectively, enabling training on small GPU clusters. However, directly deploying these solutions often leads to suboptimal efficiency. Only experienced experts can unleash the full potential of hardware by carefully tuning the distributed configuration. Thus, we present a novel solution, Elixir, which automates efficient large model training based on pre-runtime model profiling. Elixir aims to identify the optimal combination of partitioning and offloading techniques to maximize training throughput. In our experiments, Elixir significantly outperforms the current state-of-the-art baseline. Our optimal configuration achieves up to a $3.4\times$ speedup on GPT-2 models compared with SOTA solutions. We hope that our work will benefit individuals who lack computing resources and expertise, granting them access to large models¹.

1 Introduction

The current success of deep learning (DL) is attributed to the rise of pre-trained large language models (LLMs) [1, 2, 3, 4, 5, 6, 7, 8]. LLMs are widely used not only in NLP applications such as conversation, Q&A, and text generation, but also in multimodal tasks such as image generation [9, 10], and speech synthesis [11]. However, training LLMs remains challenging due to the growing size of models and limited GPU memory. In the past five years, the largest dense models have significantly increased in size, from 340 million parameters in BERT [1] to 540 billion parameters in PaLM [7]. Exerting the power of the mixture-of-experts architecture [12], the number of parameters in the largest sparse model [13] has exceeded 1 trillion. Meanwhile, GPU memory has only increased to 80GB [14, 15].

To address the memory bottleneck, researchers have proposed distributed training techniques. Distributed data parallelism (DDP) divides input data and assigns each device to compute its partition

*This work was done when Jiarui worked at HPC-AI Technology Inc.

†Dr. You is a faculty member at NUS. This work was done at HPC-AI Technology Inc.

¹The beta version of Elixir is now available at <https://github.com/hpcaitech/ColossalAI/tree/feature/elixir>

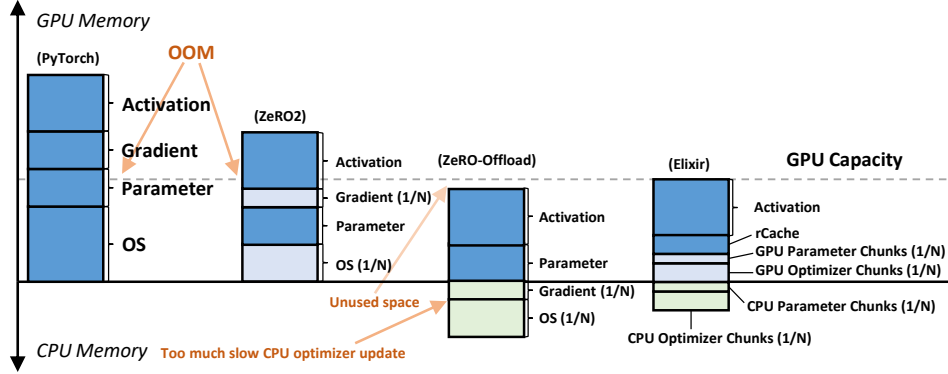


Figure 1: Comparison between Elixir and other distributed solutions.

simultaneously. Though DDP accelerates training, it requires each device to store a complete model copy. Zero Redundancy Optimizer (ZeRO) [16] is designed to eliminate memory redundancy in DDP. ZeRO partitions the model among devices, gathers parameters before computations, and scatters them afterward. The communication volume in ZeRO scales with the model size. Tensor parallelism (TP) partitions parameters used in matrix multiplication (MM) operators and replaces the original MM computation with parallel MM algorithms. Megatron-LM [17] employs an efficient TP implementation that eliminates parameter redundancy but duplicates a part of intermediate variables during training. The communication volume in this approach is determined by the size of intermediate variables, which grows linearly with batch size, sequence length, and model size. Pipeline parallelism (PP) [18, 19, 20, 21] distributes the layers of the model across compute devices, and treats the devices as a data processing pipeline. PP generally has the lowest communication costs but it brings waiting bubbles.

Though memory partitioning addresses the memory bottleneck, it requires the aggregate GPU memory to exceed the model size. Memory offloading, on the other hand, leverages next-level memory space such as CPU memory and NVMe disks to store large models when the aggregate GPU memory is insufficient. ZeRO-Infinity [22] demonstrates that memory offloading is the most promising method for scaling up models since memory and storage hardware are generally more affordable than GPUs.

ZeRO-Infinity, despite being a powerful heterogeneous training system, has two significant drawbacks: (1) ZeRO requires users to configure numerous stages and arguments. It is a rather intricate and time-consuming task to explore distributed configurations. ZeRO optimization involves 18 adjustable arguments, named *stage3_max_live_parameters*, *sub_group_size*, *round_robin_gradients*, etc., which might be unfamiliar to most AI researchers. Although DeepSpeed [23] offers an auto-tuning command, it only considers memory partitioning and does not incorporate offloading. (2) ZeRO achieves suboptimal efficiency due to a lack of awareness of the training process. By default, ZeRO-3 partitions all parameters, leading to additional communication for gathering parameters during the forward and backward pass. Similarly, its offloading option offloads all optimizer states to CPU memory, resulting in slow CPU optimizer updates for all parameters. We argue that using free GPU memory to store optimizer states or retaining gathered parameters during training can improve training throughput.

In this paper, we propose Elixir, an approach to automate large model training on a small GPU cluster. Our main goal is to make the best use of all GPU memory, maximizing the training throughput. To achieve this, we develop a pre-runtime profiler that accurately measures memory usage before training. Our profiler can profile the 175B OPT [2] model on a single A100 GPU within 10 seconds. We compact parameters into continuous blocks of the same length, called chunks, as the memory units in our parallel training system for convenience. We introduce rCache to achieve fine-grained control over the degree of memory redundancy. Therefore, we can adjust rCache size or move chunks around to utilize free GPU memory. Based on the profiling results, we analyze the benefits of these two options and identify an optimal configuration for training. In our experiments, our optimal configuration runs much faster than current SOTA solutions.

Taking Fig.1 as an example, PyTorch [24] DDP triggers a CUDA Out-Of-Memory (OOM) error in this case. Although ZeRO-2 partitions gradients and optimizer states, it still triggers an OOM error. ZeRO-Offload [25] resolves the OOM issue, but it suffers from slow CPU optimizer updates and unused CUDA memory. However, Elixir overcomes these challenges by effectively utilizing all GPU memory.

In summary, our contributions are as follows:

- We build a pre-runtime profiler designed for large models. It is capable of obtaining the computation graph and the memory usage of the model before training. We bring this powerful tool to support large model profiling.
- We introduce rCache to control the degree of memory redundancy. Moreover, we build a search engine to find the optimal configuration, maximizing training efficiency automatically. Different from previous works, our optimal configuration considers both memory partitioning and memory offloading.
- We conduct evaluations on a large scale by testing various model sizes, GPU capacities, numbers of GPUs, and batch sizes. When compared to current SOTA solutions, we observe that Elixir achieves up to $3.4\times$ acceleration without manual tuning.

2 Background: Techniques for Large Model Training

The key idea of Elixir is to intelligently manage GPU memory. We apply established techniques to reduce memory usage during training. First, we discuss how memory is consumed during training.

Memory Usage. Memory usage during training primarily consists of five components: parameters, gradients, optimizer states, activations, and buffers. Optimizer states are the extra memory footprint consumed by the optimizer. For example, Adam [26] needs to store averaged momentum and variance of gradients. We refer to parameters, gradients, and optimizer states collectively as model states. Activations are the intermediate temporary variables generated during training. Typically, activations are stored for the backward pass to compute gradients. However, their memory usage may vary depending on the training framework. In PyTorch, the temporary gradients of intermediate tensor variables can also be viewed as activations. Compared to other components, buffers consume a relatively small amount of memory. We assume that buffers are always stored in the GPU for subsequent analysis.

Mixed Precision Training [27]. The SOTA approach to train large models utilizes both the half-precision floating-point (FP16) format and the single-precision floating-point (FP32) format during training. Parameters, gradients, and activations are stored and computed in FP16 to reduce memory usage and improve efficiency. Meanwhile, the accumulation operator in the optimizer update is sensitive to underflow in low-precision formats. The master weight, which is an FP32 copy of the parameters, is used to accumulate gradients in each optimizer update and is rounded to FP16 parameters before the forward pass. In this case, the memory usage of parameters, gradients, and activations is halved, but the memory usage of optimizer states is increased due to the addition of the master weight. For example, if we use Adam and the model size is M , training requires $2M$ bytes for parameters, $2M$ bytes for gradients, and $12M$ bytes for optimizer states.

After understanding how memory is consumed during training, we discuss how to reduce the memory usage.

2.1 Reduce the Memory Usage of Model States

Model states consume a large part of memory when training large models. ZeRO and memory offloading are two effective techniques used to reduce the memory usage of model states.

ZeRO-n. ZeRO is an optimization technique for DDP. In traditional DDP, all types of memory usage, except for activations, are replicated across GPUs. ZeRO partitions model states to eliminate memory redundancy. It offers three stages for three degrees of memory partitioning. ZeRO-1 partitions optimizer states among GPUs, where each compute device only updates a partition of the model during optimizer updates. ZeRO-2 partitions gradients and optimizer states, with gradients scattered after their reduce collective communication. ZeRO-3 partitions parameters, gradients, and optimizer states, with parameters required to be gathered before computing. Thus, when ZeRO-3 is enabled,

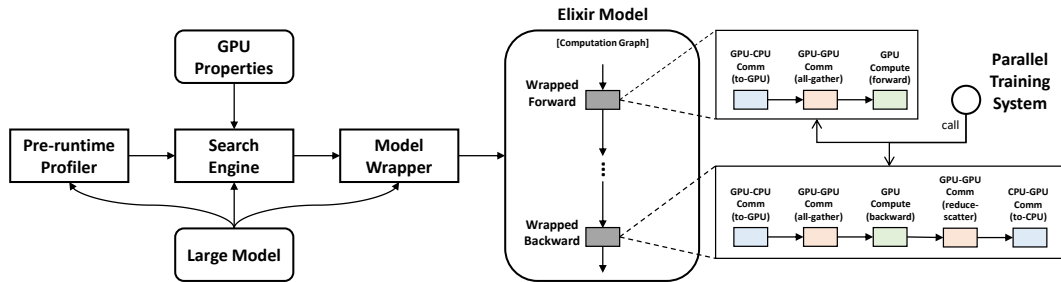


Figure 2: Coarse-grained workflow.

training on 4 GPUs only requires $\frac{1}{2}M$ bytes for parameters, $\frac{1}{2}M$ bytes for gradients, and $3M$ bytes for optimizer states on each device.

Memory Offloading. Researchers store model states in CPU memory to address the shortage of GPU memory. L2L [28] uploads each layer to the GPU before computations and offloads them to the CPU afterward. ZeRO-Offload not only utilizes CPU memory resources but also uses CPU compute resources. It offloads both optimizer states and optimizer update operators to the CPU. In the heterogeneous training paradigm proposed by ZeRO-Offload, FP16 parameters, gradients, and activations are placed in GPU memory, while FP32 optimizer states are placed in CPU memory. Before each forward pass, FP16 parameters are updated by the FP32 master weight stored in CPU. After each backward pass, FP16 gradients are transferred to CPU memory for CPU optimizer update. ZeRO-Infinity combines ZeRO-3 and memory offloading, where all model states are offloaded to CPU memory, and training only requires a buffer to store the currently computed parameters on each device.

2.2 Reduce the Memory Usage of Activations

The memory usage of activations and model states is within the same order of magnitude. However, the memory usage of activations can be significantly reduced through recomputation.

Recomputation. Activation Checkpointing (AC) [29], also known as gradient checkpointing, is a technique used to decrease the memory usage of activations. AC does not store intermediate variables in the forward pass; it recomputes the forward operators during the backward pass. Thus, the number of intermediate variables stored for the backward pass is reduced, thereby reducing the peak memory usage of activations. For instance, the 4B parameter GPT-2 model trained with a sequence length of 1K and a batch size of 2 requires 14.9GB of memory to store activations. Enabling AC reduces the memory usage of activations to 1.3GB.

3 Elixir: Overview

We propose Elixir to make hardware-efficient large model training accessible to everyone. It comprises three main components: a **pre-runtime profiler**, a **search engine**, and a **parallel training system**. The coarse-grained workflow of Elixir is quite simple (as shown in Fig.2). The pre-runtime profiler scans the given large model and generates its training information. With the knowledge of training details, the search engine identifies the optimal configuration and passes it to the model wrapper, which initializes an Elixir model according to the given configuration. All compute operators in the Elixir model are transformed into wrapped operators that automatically handle communication through the parallel training system. Before discussing more details about the components, we need to introduce some foundational concepts first.

Chunk. We borrow this concept from PatrickStar [30]. We flatten a group of parameters and concatenate them into a one-dimensional parameter with a fixed length (as shown in Fig.3 left). The insight is that one-dimensional parameters of a uniform length are more convenient to manage compared to parameters with different sizes and shapes. Moreover, we can use relatively large chunks as the communication units to fully utilize communication bandwidth.

rCache. rCache is a new memory layer allocated in GPU DRAM. We establish that only data in rCache can be duplicated across GPUs, and no other memory layers are permitted to have redundant data. In our implementation, rCache has n_{block} storage blocks of the same length to store gathered chunks. Chunks are partitioned by default in our distributed solution, we gather them into rCache before compute operators (as shown in Fig.3 right). Since the calling order of chunks can be acquired from the pre-runtime profiler, we apply Belady’s algorithm as the replacement policy of rCache.

3.1 Main Components

We take a closer look at the three main components mentioned above.

Pre-runtime Profiler. We use a pre-runtime profiler to profile the training step before running models. There are two main reasons why the profiler needs to be pre-runtime.

(1) Running large models requires complicated parallel techniques. Different types of parallelism can generate various computation graphs. Therefore, profiling large models before running them is a more robust way to collect computation graphs. (2) Dynamically allocating blocks during training leads to a large amount of memory fragmentation. For long-term active variables such as storage blocks in rCache and optimizer states, we should allocate them before training to avoid memory fragmentation. Only short-term variables such as activations should be dynamically allocated during training.

Search Engine. Based on the profiling results, an optimal configuration will be automatically found. In our implementation, the search engine needs to specify the length of chunks C , the number of blocks allocated in rCache n_{block} , and the number of chunks placed in CPU. More details about the search engine can be found in Section 5.

Parallel Training System. The parallel training system is responsible for the memory management during training. Except activations which are managed by PyTorch, parameters, gradients, and optimizer states are managed by Elixir. In our implementation, we wrap all compute operators with GPU-GPU and GPU-CPU communication to ensure that parameters are complete before computations and gradients are partitioned after reduction communications.

4 Elixir: Cost Analysis

We analyze the memory usage and communication volume of our parallel training strategy, showing that it can achieve comparable results to ZeRO-2 and ZeRO-3 when the configuration is at the boundary points. Furthermore, we demonstrate how Elixir finds opportunities for optimization. In our analysis, we define the following variables: N as the number of GPUs, M as the model size, L_c as the precision length in computations, L_{os} as the precision length in optimizer updates, and F_{os} as the additional memory overhead of the optimizer, C as the chunk length, $S = n_{\text{block}}C$ as the aggregate length of chunks. In practice, the waste rate caused by packaging all the parameters into chunks is less than 4%, so we assume $S \approx M$.

4.1 Total Memory Usage of a Chunk

We create two chunks for the same group of parameters: the parameter chunk and the optimizer chunk, which are used for computation and optimizer updates, respectively. We omit gradient chunks because we reuse parameter chunks to store gradients [30]. As the gradient of a parameter has the same size as its data, we replace the data of each parameter in the parameter chunk with its generated gradient (as shown in Fig.3 center). Once all the parameters within a chunk have completed gradient calculations, that chunk is transformed into a gradient chunk. We utilize the transformed parameter chunk and optimizer chunk to perform one optimizer update, so each parameter chunk and its paired optimizer chunk must be stored on the same device. In summary, the total memory usage of a chunk is $\frac{L_c C + L_{os} F_{os} C}{N}$.

4.2 Compared with ZeRO

We demonstrate the memory usage and communication volume of various distributed parallel training strategies in Table 1, where activation checkpointing is enabled. The rCache-max strategy is

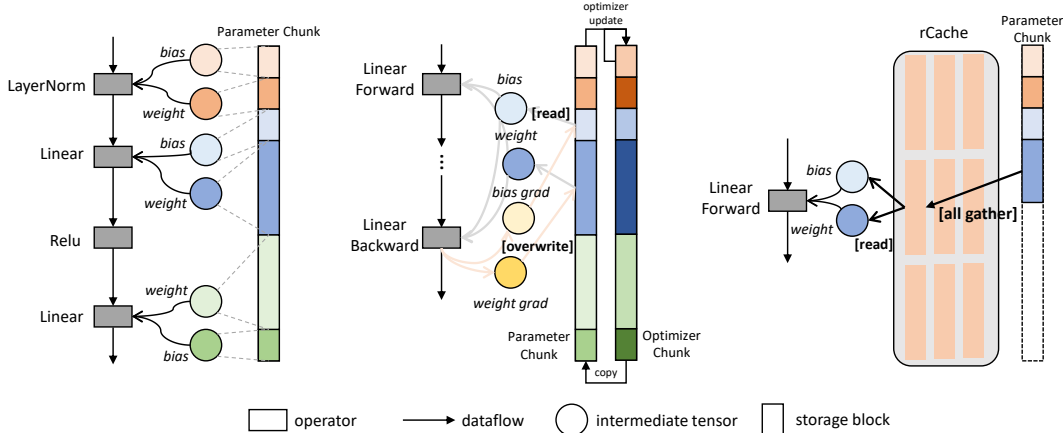


Figure 3: Left: The data of each parameter is compacted into a parameter chunk. Center: During the forward and backward pass, each operator reads the data of relevant parameters from their corresponding parameter chunks. Once the gradient calculation of a parameter is finished, it is no longer used in subsequent operators. We use the gradient to overwrite the data in the parameter chunk. Right: Chunks should be gathered in rCache before reading their data. After the backward pass, chunks should be scattered and then used to update its distributed shards.

Table 1: Memory usage and communication volume of different parallel distributed strategies. ϵ is the size of a buffer used to store gathered parameters.

Name	GPU Memory (per GPU)	GPU-CPU Comm	GPU-GPU Comm
DDP	$(L_c + L_c + L_{os}F_{os})M$	0	$2L_cM$
ZeRO-1	$(L_c + L_c)M + \frac{(L_{os}F_{os})M}{N}$	0	$2L_cM$
ZeRO-2 \rightarrow offload	$L_cM + \frac{(L_c + L_{os}F_{os})M}{N} \rightarrow L_cM$	$0 \rightarrow 2L_cM$	$2L_cM$
ZeRO-3 \rightarrow offload	$\frac{(L_c + L_c + L_{os}F_{os})M}{N} \rightarrow \epsilon$	$0 \rightarrow 4L_cM$	$4L_cM$
rCache-max \rightarrow offload	$L_cS + \frac{(L_c + L_{os}F_{os})S}{N} \rightarrow L_cS$	$0 \rightarrow 2L_cS$	$2L_cS$
rCache-min \rightarrow offload	$L_cC + \frac{(L_c + L_{os}F_{os})S}{N} \rightarrow L_cC$	$0 \rightarrow 4L_cS$	$4L_cS$

comparable to ZeRO-2. It sets n_{blocks} to its maximum number, n_{chunks} , resulting in each chunk only being gathered in the forward pass and reduced in the backward pass. The rCache-min strategy is comparable to ZeRO-3. The rCache-min strategy limits n_{blocks} to its minimum number, 1, allowing only one chunk to be gathered during the training step. In the context of training a large model on a small cluster, we assume that $n_{\text{chunks}} > N$, where we have $C < \frac{M}{N}$. When the rCache size is set between the minimum and maximum values, the memory usage is between that of rCache-min and rCache-max, and the communication volume is between that of rCache-max and rCache-min. In this way, Elixir trades off memory usage and communication volume to utilize free GPU memory.

When the offloading option is enabled, we observe that the GPU-CPU communication volume remains the same as the GPU-CPU communication volume. It should be noted that ZeRO-3 Offload and rCache-min Offload do not have the same memory usage. In practice, we have found that the latter one utilizes less GPU memory. Similarly, Elixir can also trade off memory usage and CPU optimizer updates to improve efficiency.

4.3 Communication Overlap

We asynchronously prefetch the next-used chunk based on the calling order of chunks from the pre-runtime profiler. By using streams concurrently, we can overlap the all-gather communication in prefetch operations with the computation of currently active chunks in rCache. We assume that communication is not a bottleneck for efficiency and can be perfectly overlapped with computation

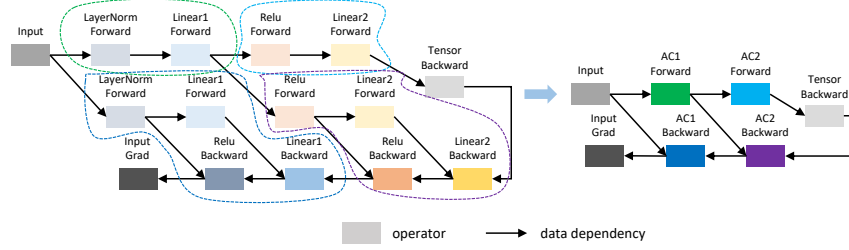


Figure 4: In the left graph, each parameter is called twice in the forward functions and once in the backward functions, resulting in an uncommon computation graph. In the right graph, we consider the AC function as an operator, and each parameter is only called once in the backward pass.

when training on a small cluster. Therefore, GPU-GPU communication is not included in the subsequent configuration search analysis.

5 Elixir: Find the Optimal Configuration

The search engine utilizes the profiling results from the pre-runtime profiler to identify an optimal configuration. The engine obtains the allowed memory usage, denoted as U_{allowed} , and finds the optimal chunk length C (See more details in Appendix.A).

5.1 Optimal Offloading Configuration

We approach finding the optimal configuration as an optimization problem. Initially, we set the size of rCache to 1 and offload all chunks to CPU memory. Our goal is to maximize training throughput within a budget of U_{allowed} . There are two options for utilizing the available GPU memory. The first option is to expand the rCache size to cache more recently used chunks. The second option is to upload chunks and their optimizer updates to GPUs. We analyze the benefits of both options.

We introduce the definition of the common computation graph (as shown in Fig.4 right). In most LLM implementations, each parameter is called once during the forward pass and once during the backward pass, except for the weight in the embedding layer. The calling order of parameters in the backward pass is exactly the reverse of the calling order in the forward pass.

The computation graph is no longer common when activation checkpointing (AC) is enabled, as each parameter is called twice in the backward pass (as shown in Fig.4 left). To address this, we consider the computation graph from a coarse-grained perspective, treating an AC function as a compute operator. As shown in Fig.4, we transform an uncommon computation graph into a common computation graph.

Our strategy is to extend rCache to ensure that it is large enough to cache all the chunks used in each coarse-grained compute operator (See more details in Appendix.A.3). Therefore, we have the following observations: (1) Each chunk is gathered once into rCache in the forward pass and once in the backward pass. (2) In the backward pass, the order of replicated chunks is the exact reverse of the order in the forward pass.

We define the following variables to analyze the benefits: $B_{g2c}(n)$ and $B_{c2g}(n)$ represent the aggregate communication bandwidth of n processes when transferring data from GPU to CPU and from CPU to GPU, respectively. $V_g(n)$ and $V_c(n)$ represent the aggregate update velocity with n processes on GPU and CPU, respectively.

$$I(n) = \frac{1}{L_c} \left(\frac{L_c C}{B_{g2c}(n)} + \frac{L_c C}{B_{c2g}(n)} \right) \quad (1)$$

We analyze the time saved when extending a single storage block for rCache. With one more storage block available, rCache is able to cache one more chunk at the end of the forward pass. This cached chunk does not require extra offloading communication in the backward pass. The normalized benefit is denoted as $I(n)$.

$$J(n) = \frac{n}{L_c + L_{os}F_{os}} \left[\left(\frac{L_{os}C}{B_{c2g}(n)} + L_c I(n) + \frac{L_c C}{B_{g2c}(n)} \right) + \left(\frac{C}{V_c(n)} - \frac{C}{V_g(n)} \right) \right] \quad (2)$$

We analyze the time saved when uploading a chunk to the GPU. We eliminate offloading communication for this chunk and replace its CPU optimizer update with a GPU optimizer update. The normalized benefit is denoted as $J(n)$.

We can compare $I(n)$ and $J(n)$ to determine whether to prioritize uploading chunks or expanding rCache. For instance, if $J(n) > I(n)$, we should prioritize uploading as many chunks as possible. If there is still available space, we can then shift our focus to extending rCache.

6 Experiments

We evaluate the performance of using Elixir to train GPT models on various training configurations¹. We observe that Elixir runs faster than existing SOTA solutions: up to $3.4\times$ speedup on A100 80GB, and $3\times$ speedup on A100 40GB (see Appendix.C).

6.1 Experiments Settings

We conducted our experiments using two types of A100 compute nodes. One type is equipped with 4 A100 80GB PCIe GPUs and 400GiB CPU DRAM. The other type has 4 A100 40GB SXM GPUs, NVLink [31], and 500GiB CPU DRAM. See Appendix.B.1 for more details about the hardware performance.

We exclusively evaluate GPT-2 models, as large language models typically share the same transformer [32] architecture as GPT-2. We vary the model size, batch size, number of GPUs, and GPU capacity to assess how the performance changes across different training configurations. Activation checkpointing and mixed-precision training are enabled in our experiments. To measure training efficiency, we utilize TFLOPS as the metric, which is defined as $8MD$ [33], where M represents the model size and D represents the number of tokens.

Our baselines include Megatron-LM, FSDP [34], and DeepSpeed. We do not include PP because it is commonly employed across compute nodes [20]. The training efficiency of DeepSpeed is measured as the highest throughput selected from ZeRO-2, ZeRO-2 Offload, ZeRO-3, and ZeRO-3 Offload. Notice that GPT-2 models evaluated with Elixir, FSDP, and DeepSpeed are sourced from HuggingFace [35], while GPT-2 models evaluated with Megatron are implemented by itself. We also apply FlashAttention [36] in GPT-2 models.

6.2 Experiments Results

Our experiments focus on validating the robustness of Elixir. We vary the training arguments to modify the memory usage settings, including using different model sizes to adjust the memory usage of model states, varying GPU capacities and the number of GPUs to modify the aggregate GPU memory size, and utilizing various batch sizes to alter the memory usage of activations. The complete results can be found in Appendix.C. Here, we have selected a representative subset of the data for analysis.

Increasing the Model Size. The results are presented in Table 2 which demonstrates the impact of increasing the memory usage of model states. Megatron and FSDP encounter OOM errors in most cases due to their requirement for a large aggregate GPU memory space. DeepSpeed can consistently train large models, partly because it is measured across four distributed configurations. Elixir not only avoids OOM errors during training but also achieves the highest throughput. On A100 40GB, Elixir achieves $2\times$ speedup in most cases. On A100 80GB, Elixir also achieves up to $2\times$ speedup.

We observe that Elixir achieves less speedup on small models or GPUs with more memory space, as the aggregate GPU memory is sufficient when training small models or with an abundance of GPUs. In this case, memory offloading is not necessary, and current SOTA solutions have nearly reached optimal efficiency.

¹The benchmark code is available at <https://github.com/hpcaitech/Elixir>

Table 2: The profiled training efficiency (TFLOPS) when the batch size per GPU is set to 8.

Number of GPUs	Model	A100 40GB SXM				A100 80GB PCIe			
		Elixir	Megatron	FSDP	DeepSpeed	Elixir	Megatron	FSDP	DeepSpeed
1	4b	82	OOM	OOM	46	147	155	148	140
	10b	66	OOM	OOM	46	84	OOM	OOM	58
	15b	77	OOM	OOM	37	77	OOM	OOM	62
	20b	69	OOM	OOM	36	73	OOM	OOM	30
2	4b	152	OOM	OOM	125	150	148	144	144
	10b	91	OOM	OOM	55	145	OOM	OOM	72
	15b	96	OOM	OOM	55	104	OOM	OOM	83
	20b	89	OOM	OOM	46	101	OOM	OOM	48
4	4b	157	129	131	153	137	97	130	131
	10b	138	OOM	OOM	60	145	116	OOM	130
	15b	129	OOM	OOM	62	150	138	OOM	148
	20b	123	OOM	OOM	60	139	OOM	OOM	OOM

We also observe that the training efficiency drops when increasing the model size, because memory offloading brings extra communication between the CPU and GPUs. Elixir is able to alleviate this negative impact when there are more GPUs. While DeepSpeed has significant performance drop when increasing the model size due to the change of the used distributed solution. This observation proves that Elixir utilizes GPU memory more intelligently.

Table 3: The profiled training efficiency (TFLOPS) when the number of GPUs is set to 4. Due to the lack of CPU memory on the A100 80GB compute node, DeepSpeed occurs OOM error when training the 20b GPT-2 model.

model	batch size	A100 40GB SXM				A100 80GB PCIe			
		Elixir	Megatron	FSDP	DeepSpeed	Elixir	Megatron	FSDP	DeepSpeed
4b	4	144	123	131	139	114	79	106	109
	12	164	107	OOM	153	147	99	141	140
	16	167	OOM	OOM	164	154	99	146	147
10b	4	112	OOM	OOM	36	124	112	OOM	108
	12	136	OOM	OOM	77	153	113	OOM	146
	16	151	OOM	OOM	91	164	105	OOM	158
15b	4	97	OOM	OOM	34	126	142	OOM	117
	12	144	OOM	OOM	82	167	138	OOM	163
	16	150	OOM	OOM	102	175	OOM	OOM	164
20b	4	91	OOM	OOM	33	102	OOM	OOM	OOM
	12	141	OOM	OOM	79	151	OOM	OOM	OOM
	16	146	OOM	OOM	95	161	OOM	OOM	OOM

Increasing the Batch Size. We increase the batch size to increase the memory usage of activations, and the profiled results is shown in Table 3. For Elixir, FSDP, and DeepSpeed, their training throughput become higher when increasing the batch size. Meanwhile, the training throughput of Megatron keeps the same. The reason is that the communication volume of the previous three solutions is the model size but the communication volume of Megatron increases linearly with the batch size.

We observe that the speedup ratio of Elixir to DeepSpeed becomes smaller when increasing the batch size. There are two aspects to explain this phenomenon. Increasing the batch size increases the memory usage of activations and the time elapsed on the computation. Thus, there is no enough available GPU memory for Elixir to arrange. Also, the proportion of computation time increases, making the optimization in communications and CPU computations less effective. Despite these limitations, Elixir still achieves a $1.5\times$ speedup on A100 40GB.

7 Limitations

We focus on small GPU clusters, and our research does not involve large-scale model training. Current research suggests that using the complicated combined parallelism plans is a better choice than relying only one distributed solution when training on a large network with intricate communication topology [20, 37].

8 Conclusion

Large model training becomes a fundamental approach widely applied in DL domains. Memory partitioning and memory offloading are necessary techniques to train large models on limited compute devices. Thus, automating the offloading training is the key to truly make the large model training accessible to everyone. To the best of our knowledge, we are the first to consider both partitioning and offloading together and achieve the optimal configuration within our search space. Our findings suggest that using a dynamic distributed strategy based on profiling results can result in tripled throughput compared to a rigid distributed strategy. We hope that our work can assist the majority of AI researchers.

References

- [1] Jacob Devlin, Ming-Wei Chang, Kenton Lee, and Kristina Toutanova. Bert: Pre-training of deep bidirectional transformers for language understanding. *arXiv preprint arXiv:1810.04805*, 2018.
- [2] Susan Zhang, Stephen Roller, Naman Goyal, Mikel Artetxe, Moya Chen, Shuohui Chen, Christopher Dewan, Mona Diab, Xian Li, Xi Victoria Lin, et al. Opt: Open pre-trained transformer language models. *arXiv preprint arXiv:2205.01068*, 2022.
- [3] Alec Radford, Jeffrey Wu, Rewon Child, David Luan, Dario Amodei, Ilya Sutskever, et al. Language models are unsupervised multitask learners. *OpenAI blog*, 1(8):9, 2019.
- [4] Tom Brown, Benjamin Mann, Nick Ryder, Melanie Subbiah, Jared D Kaplan, Prafulla Dhariwal, Arvind Neelakantan, Pranav Shyam, Girish Sastry, Amanda Askell, et al. Language models are few-shot learners. *Advances in neural information processing systems*, 33:1877–1901, 2020.
- [5] OpenAI. Gpt-4 technical report. *ArXiv*, abs/2303.08774, 2023.
- [6] Teven Le Scao, Angela Fan, Christopher Akiki, Ellie Pavlick, Suzana Ilić, Daniel Hesslow, Roman Castagné, Alexandra Sasha Luccioni, François Yvon, Matthias Gallé, et al. Bloom: A 176b-parameter open-access multilingual language model. *arXiv preprint arXiv:2211.05100*, 2022.
- [7] Aakanksha Chowdhery, Sharan Narang, Jacob Devlin, Maarten Bosma, Gaurav Mishra, Adam Roberts, Paul Barham, Hyung Won Chung, Charles Sutton, Sebastian Gehrmann, et al. Palm: Scaling language modeling with pathways. *arXiv preprint arXiv:2204.02311*, 2022.
- [8] Romal Thoppilan, Daniel De Freitas, Jamie Hall, Noam Shazeer, Apoorv Kulshreshtha, Heng-Tze Cheng, Alicia Jin, Taylor Bos, Leslie Baker, Yu Du, et al. Lamda: Language models for dialog applications. *arXiv preprint arXiv:2201.08239*, 2022.
- [9] Jiahui Yu, Yuanzhong Xu, Jing Yu Koh, Thang Luong, Gunjan Baid, Zirui Wang, Vijay Vasudevan, Alexander Ku, Yinfei Yang, Burcu Karagol Ayan, et al. Scaling autoregressive models for content-rich text-to-image generation. *arXiv preprint arXiv:2206.10789*, 2022.
- [10] Huiwen Chang, Han Zhang, Jarred Barber, AJ Maschinot, Jose Lezama, Lu Jiang, Ming-Hsuan Yang, Kevin Murphy, William T Freeman, Michael Rubinstein, et al. Muse: Text-to-image generation via masked generative transformers. *arXiv preprint arXiv:2301.00704*, 2023.
- [11] Chengyi Wang, Sanyuan Chen, Yu Wu, Ziqiang Zhang, Long Zhou, Shujie Liu, Zhuo Chen, Yanqing Liu, Huaming Wang, Jinyu Li, et al. Neural codec language models are zero-shot text to speech synthesizers. *arXiv preprint arXiv:2301.02111*, 2023.
- [12] Noam Shazeer, Azalia Mirhoseini, Krzysztof Maziarz, Andy Davis, Quoc Le, Geoffrey Hinton, and Jeff Dean. Outrageously large neural networks: The sparsely-gated mixture-of-experts layer. *arXiv preprint arXiv:1701.06538*, 2017.
- [13] William Fedus, Barret Zoph, and Noam Shazeer. Switch transformers: Scaling to trillion parameter models with simple and efficient sparsity. *The Journal of Machine Learning Research*, 23(1):5232–5270, 2022.

- [14] NVIDIA. Nvidia a100 tensor core gpu architecture, 2020.
- [15] NVIDIA. Nvidia h100 tensor core gpu architecture, 2022.
- [16] Samyam Rajbhandari, Jeff Rasley, Olatunji Ruwase, and Yuxiong He. Zero: Memory optimizations toward training trillion parameter models. In *SC20: International Conference for High Performance Computing, Networking, Storage and Analysis*, pages 1–16. IEEE, 2020.
- [17] Mohammad Shoeybi, Mostofa Patwary, Raul Puri, Patrick LeGresley, Jared Casper, and Bryan Catanzaro. Megatron-lm: Training multi-billion parameter language models using model parallelism. *arXiv preprint arXiv:1909.08053*, 2019.
- [18] Yanping Huang, Youlong Cheng, Ankur Bapna, Orhan Firat, Dehao Chen, Mia Chen, HyoukJoong Lee, Jiquan Ngiam, Quoc V Le, Yonghui Wu, et al. Gpipe: Efficient training of giant neural networks using pipeline parallelism. *Advances in neural information processing systems*, 32, 2019.
- [19] Deepak Narayanan, Aaron Harlap, Amar Phanishayee, Vivek Seshadri, Nikhil R Devanur, Gregory R Ganger, Phillip B Gibbons, and Matei Zaharia. Pipedream: Generalized pipeline parallelism for dnn training. In *Proceedings of the 27th ACM Symposium on Operating Systems Principles*, pages 1–15, 2019.
- [20] Deepak Narayanan, Mohammad Shoeybi, Jared Casper, Patrick LeGresley, Mostofa Patwary, Vijay Korthikanti, Dmitri Vainbrand, Prethvi Kashinkunti, Julie Bernauer, Bryan Catanzaro, et al. Efficient large-scale language model training on gpu clusters using megatron-lm. In *Proceedings of the International Conference for High Performance Computing, Networking, Storage and Analysis*, pages 1–15, 2021.
- [21] Shigang Li and Torsten Hoefler. Chimera: efficiently training large-scale neural networks with bidirectional pipelines. In *Proceedings of the International Conference for High Performance Computing, Networking, Storage and Analysis*, pages 1–14, 2021.
- [22] Samyam Rajbhandari, Olatunji Ruwase, Jeff Rasley, Shaden Smith, and Yuxiong He. Zero-infinity: Breaking the gpu memory wall for extreme scale deep learning. In *Proceedings of the International Conference for High Performance Computing, Networking, Storage and Analysis*, pages 1–14, 2021.
- [23] Jeff Rasley, Samyam Rajbhandari, Olatunji Ruwase, and Yuxiong He. Deepspeed: System optimizations enable training deep learning models with over 100 billion parameters. In *Proceedings of the 26th ACM SIGKDD International Conference on Knowledge Discovery & Data Mining*, pages 3505–3506, 2020.
- [24] Adam Paszke, Sam Gross, Francisco Massa, Adam Lerer, James Bradbury, Gregory Chanan, Trevor Killeen, Zeming Lin, Natalia Gimelshein, Luca Antiga, et al. Pytorch: An imperative style, high-performance deep learning library. *Advances in neural information processing systems*, 32, 2019.
- [25] Jie Ren, Samyam Rajbhandari, Reza Yazdani Aminabadi, Olatunji Ruwase, Shuangyan Yang, Minjia Zhang, Dong Li, and Yuxiong He. Zero-offload: Democratizing billion-scale model training. In *USENIX Annual Technical Conference*, pages 551–564, 2021.
- [26] Diederik P Kingma and Jimmy Ba. Adam: A method for stochastic optimization. *arXiv preprint arXiv:1412.6980*, 2014.
- [27] Paulius Micikevicius, Sharan Narang, Jonah Alben, Gregory Diamos, Erich Elsen, David Garcia, Boris Ginsburg, Michael Houston, Oleksii Kuchaiev, Ganesh Venkatesh, et al. Mixed precision training. *arXiv preprint arXiv:1710.03740*, 2017.
- [28] Bharadwaj Pudipeddi, Maral Mesmakhosroshahi, Jinwen Xi, and Sujeeth Bharadwaj. Training large neural networks with constant memory using a new execution algorithm. *arXiv preprint arXiv:2002.05645*, 2020.
- [29] Tianqi Chen, Bing Xu, Chiyuan Zhang, and Carlos Guestrin. Training deep nets with sublinear memory cost. *arXiv preprint arXiv:1604.06174*, 2016.

- [30] Jiarui Fang, Zilin Zhu, Shenggui Li, Hui Su, Yang Yu, Jie Zhou, and Yang You. Parallel training of pre-trained models via chunk-based dynamic memory management. *IEEE Transactions on Parallel and Distributed Systems*, 34(1):304–315, 2022.
- [31] Nvlink and nvswitch. <https://www.nvidia.com/en-us/data-center/nvlink/>.
- [32] Ashish Vaswani, Noam Shazeer, Niki Parmar, Jakob Uszkoreit, Llion Jones, Aidan N Gomez, Łukasz Kaiser, and Illia Polosukhin. Attention is all you need. *Advances in neural information processing systems*, 30, 2017.
- [33] Jared Kaplan, Sam McCandlish, Tom Henighan, Tom B Brown, Benjamin Chess, Rewon Child, Scott Gray, Alec Radford, Jeffrey Wu, and Dario Amodei. Scaling laws for neural language models. *arXiv preprint arXiv:2001.08361*, 2020.
- [34] Yanli Zhao, Andrew Gu, Rohan Varma, Liang Luo, Chien-Chin Huang, Min Xu, Less Wright, Hamid Shojanazeri, Myle Ott, Sam Shleifer, et al. Pytorch fsdp: Experiences on scaling fully sharded data parallel. *arXiv preprint arXiv:2304.11277*, 2023.
- [35] Thomas Wolf, Lysandre Debut, Victor Sanh, Julien Chaumond, Clement Delangue, Anthony Moi, Pierric Cistac, Tim Rault, Rémi Louf, Morgan Funtowicz, et al. Transformers: State-of-the-art natural language processing. In *Proceedings of the 2020 conference on empirical methods in natural language processing: system demonstrations*, pages 38–45, 2020.
- [36] Tri Dao, Dan Fu, Stefano Ermon, Atri Rudra, and Christopher Ré. Flashattention: Fast and memory-efficient exact attention with io-awareness. *Advances in Neural Information Processing Systems*, 35:16344–16359, 2022.
- [37] Lianmin Zheng, Zhuohan Li, Hao Zhang, Yonghao Zhuang, Zhifeng Chen, Yanping Huang, Yida Wang, Yuanzhong Xu, Danyang Zhuo, Eric P Xing, et al. Alpa: Automating inter-and {Intra-Operator} parallelism for distributed deep learning. In *16th USENIX Symposium on Operating Systems Design and Implementation (OSDI 22)*, pages 559–578, 2022.

A Algorithm Details

A.1 Allowed Memory Usage

The search engine depends on the allowed memory usage, denoted as U_{allowed} .

$$U_{\text{allowed}} = F_{\text{alloc}} \cdot \left(\text{capacity}_{\text{gpu}} - U_{\text{buffer}} - F_{\text{frag}} \cdot U_{\text{activation}} \right)$$

In the equation, U_{buffer} and $U_{\text{activation}}$ represent the memory usage of buffers and activations, respectively. We receive these two variables from the pre-runtime profiler. Due to the impact of generated memory fragments during training, we must reserve additional GPU memory for activations. To account for this reservation, we multiply the memory usage of activations by a ratio greater than 1, denoted as F_{frag} . The value of F_{alloc} is used to estimate the proportion of GPU memory that Elixir can effectively use. By default, F_{alloc} is set to 0.95, and F_{frag} is set to 1.25.

A.2 Grouping Method and Optimal Chunk Size

For a given chunk size, we sort all parameters into a sequence based on their order of use during the forward pass, assuming that each parameter is used only once. Parameters used multiple times, such as the weight of the embedding layer, are rare in language models, and we handle them by using ZeRO-2. We iterate through this sequence, maintaining a current chunk and attempting to group each parameter with its preceding parameter. If the current chunk is insufficient for the parameter, we close it and assign a new chunk.

We define the optimal chunk size as the size that minimizes the total number of bytes replaced in rCache during one training step. To determine this size, we simulate various chunk sizes, calculate the number of replacements for each, and select the best value. To search more values within a given time, we implement the simulation algorithm in C++ for better efficiency.

A.3 Activation Checkpointing Detector

We detect the parameters accessed by each activation checkpointing (AC) function using the pre-runtime profiler. We define the buffer size of AC as the maximum summation of the number of elements in all parameters accessed by each AC function. The first priority of Elixir is to ensure that the rCache size is greater than the buffer size of AC. If U_{allowed} is smaller than the buffer size of AC, we extend rCache as much as possible and keep all chunks in CPU memory.

B Experiments Details

B.1 Hardware Performance

We profiled the hardware performance on our development server and AWS cloud server. The results are shown in Table 4 and Table 5. Additionally, the hardware performance on NSCC is similar to our development server, with the exception that the 4 GPUs are linked by high-bandwidth NVLINK, reaching 200GB/s. Comparing the two tables, we observe that the communication bandwidth between the GPU and CPU on AWS is significantly lower. When comparing the two tables, we observe a difference in the communication bandwidth between the GPU and CPU on AWS, which is notably lower. Consequently, memory offloading leads to a performance drop on AWS.

Table 4: Hardware performance (GB/s) profiled on our development server.

n	$B_{g2g}(n)$	Development Server			
		$B_{c2g}(n)$	$B_{g2c}(n)$	$V_g(n)$	$V_c(n)$
1	-	22	16	50	5
2	201	50	40	100	6.5
4	58	70	60	200	7.5

Table 5: Hardware performance (GB/s) profiled on an p4d.24xlarge instance provided by AWS.

n	AWS Cloud Server				
	$B_{g2g}(n)$	$B_{c2g}(n)$	$B_{g2c}(n)$	$V_g(n)$	$V_c(n)$
1	-	12	13	44	3.7
2	188	12	13	86	5.6
4	214	25	26	171	5

B.2 Model Configurations

GPT-2 model configurations are shown in Table 6.

Table 6: GPT-2 model configurations.

name	hidden size	num layer	num attention heads
GPT2-4b	3072	32	24
GPT2-10b	4096	48	32
GPT2-15b	8192	18	64
GPT2-20b	8192	24	64

C Full Experimental Results

The complete experimental results are presented in Table 7 and Table 8. Elixir achieves a speedup of up to 3x on A100 40GB and 3.4x on A100 80GB.

Table 7: Experimental results (TFLOPS) on A100 40GB.

M	n	bs	Elixir	Megatron	FSDP	DS-Z2	DS-Z3	DS-Z2-o	DS-Z3-o	speedup
4	1	4	62.0	OOM	OOM	OOM	OOM	26.4	19.4	2.35x
		8	82.7	OOM	OOM	OOM	OOM	46.3	40.5	1.79x
		12	102.5	OOM	OOM	OOM	OOM	64.3	50.7	1.59x
		16	113.3	OOM	OOM	OOM	OOM	77.6	60.6	1.46x
	2	4	137.3	138.0	OOM	OOM	102.0	33.8	25.7	0.99x
		8	152.2	OOM	OOM	OOM	125.7	53.3	46.0	1.21x
		12	148.5	OOM	OOM	OOM	OOM	73.6	64.3	2.02x
		16	145.8	OOM	OOM	OOM	OOM	81.0	75.4	1.8x
	4	4	144.6	123.8	131.2	137.1	139.9	34.1	28.9	1.03x
		8	157.7	130.0	131.3	153.2	152.4	60.7	54.8	1.03x
		12	164.3	107.1	OOM	161.4	160.1	77.4	69.4	1.02x
		16	167.1	OOM	OOM	164.9	162.5	91.4	89.2	1.01x
10	1	4	47.9	OOM	OOM	OOM	OOM	27.6	21.1	1.73x
		8	66.5	OOM	OOM	OOM	OOM	46.5	39.1	1.43x
		12	88.0	OOM	OOM	OOM	OOM	60.7	54.8	1.45x
		16	98.7	OOM	OOM	OOM	OOM	80.7	65.9	1.22x
	2	4	64.6	OOM	OOM	OOM	OOM	30.3	26.3	2.14x
		8	91.2	OOM	OOM	OOM	OOM	55.9	49.0	1.63x
		12	103.8	OOM	OOM	OOM	OOM	70.6	62.8	1.47x
		16	118.3	OOM	OOM	OOM	OOM	80.4	75.6	1.47x
	4	4	112.6	OOM	OOM	OOM	OOM	36.5	31.9	3.09x
		8	138.4	OOM	OOM	OOM	OOM	60.3	55.3	2.3x
		12	136.3	OOM	OOM	OOM	OOM	78.0	75.2	1.75x
		16	151.7	OOM	OOM	OOM	OOM	92.0	88.8	1.65x
15	1	4	42.0	OOM	OOM	OOM	OOM	OOM	19.2	2.19x
		8	77.6	OOM	OOM	OOM	OOM	OOM	37.1	2.09x
		12	93.6	OOM	OOM	OOM	OOM	OOM	63.4	1.48x
		16	107.8	OOM	OOM	OOM	OOM	OOM	64.6	1.67x
	2	4	59.7	OOM	OOM	OOM	OOM	OOM	27.0	2.21x
		8	96.4	OOM	OOM	OOM	OOM	OOM	55.7	1.73x
		12	109.7	OOM	OOM	OOM	OOM	OOM	69.6	1.58x
		16	128.5	OOM	OOM	OOM	OOM	OOM	87.3	1.47x
	4	4	97.7	OOM	OOM	OOM	OOM	OOM	35.0	2.79x
		8	129.1	OOM	OOM	OOM	OOM	OOM	62.8	2.05x
		12	144.3	OOM	OOM	OOM	OOM	OOM	82.2	1.76x
		16	151.0	OOM	OOM	OOM	OOM	OOM	102.5	1.47x
20	1	4	42.0	OOM	OOM	OOM	OOM	OOM	18.9	2.22x
		8	69.4	OOM	OOM	OOM	OOM	OOM	36.6	1.9x
		12	86.2	OOM	OOM	OOM	OOM	OOM	48.8	1.77x
		16	108.4	OOM	OOM	OOM	OOM	OOM	63.2	1.71x
	2	4	55.5	OOM	OOM	OOM	OOM	OOM	25.0	2.22x
		8	89.0	OOM	OOM	OOM	OOM	OOM	47.0	1.89x
		12	113.6	OOM	OOM	OOM	OOM	OOM	64.5	1.76x
		16	130.5	OOM	OOM	OOM	OOM	OOM	78.1	1.67x
	4	4	91.8	OOM	OOM	OOM	OOM	OOM	33.6	2.73x
		8	124.0	OOM	OOM	OOM	OOM	OOM	60.2	2.06x
		12	141.2	OOM	OOM	OOM	OOM	OOM	79.4	1.78x
		16	146.5	OOM	OOM	OOM	OOM	OOM	95.1	1.54x

Table 8: Experimental results (TFLOPS) on A100 80GB.

M	n	bs	Elixir	Megatron	FSDP	DS-Z2	DS-Z3	DS-Z2-o	DS-Z3-o	speedup
4	1	4	131.7	140.5	135.3	OOM	122.6	32.2	16.0	0.94x
		8	147.1	155.8	148.3	OOM	140.3	54.1	28.6	0.94x
		12	155.0	166.6	155.6	OOM	150.0	86.1	45.5	0.93x
		16	158.4	167.7	158.3	OOM	155.3	82.4	53.9	0.94x
	2	4	136.5	137.6	130.1	126.8	129.1	35.3	27.3	0.99x
		8	150.6	149.0	144.5	144.0	143.7	72.5	41.1	1.01x
		12	157.4	153.1	152.6	152.8	151.5	84.8	59.8	1.03x
		16	161.4	152.5	155.6	156.5	154.5	89.7	69.7	1.03x
	4	4	114.4	79.0	106.5	92.0	109.4	38.3	27.7	1.05x
		8	137.4	98.0	131.0	119.2	131.6	59.5	52.2	1.04x
		12	147.9	99.2	141.3	133.4	140.1	78.7	67.2	1.05x
		16	155.0	99.2	146.3	141.2	147.5	89.0	90.6	1.05x
10	1	4	56.0	OOM	OOM	OOM	OOM	33.9	14.1	1.65x
		8	84.8	OOM	OOM	OOM	OOM	58.6	29.1	1.45x
		12	102.1	OOM	OOM	OOM	OOM	73.1	43.9	1.4x
		16	110.3	OOM	OOM	OOM	OOM	88.7	55.0	1.24x
	2	4	130.3	OOM	OOM	OOM	OOM	38.4	26.1	3.39x
		8	145.6	OOM	OOM	OOM	OOM	72.8	46.7	2.0x
		12	144.4	OOM	OOM	OOM	OOM	88.8	62.8	1.63x
		16	154.9	OOM	OOM	OOM	OOM	108.0	66.5	1.43x
	4	4	124.8	112.8	OOM	OOM	108.8	40.8	29.4	1.11x
		8	145.5	116.1	OOM	OOM	140.4	65.0	57.5	1.04x
		12	153.2	113.7	OOM	OOM	146.2	86.4	71.9	1.05x
		16	164.3	105.8	OOM	OOM	158.2	89.4	87.0	1.04x
15	1	4	47.6	OOM	OOM	OOM	OOM	36.7	18.9	1.3x
		8	77.3	OOM	OOM	OOM	OOM	62.3	30.1	1.24x
		12	94.2	OOM	OOM	OOM	OOM	82.1	41.1	1.15x
		16	108.9	OOM	OOM	OOM	OOM	98.6	57.2	1.1x
	2	4	90.0	OOM	OOM	OOM	OOM	40.3	29.8	2.23x
		8	104.3	OOM	OOM	OOM	OOM	83.0	47.5	1.26x
		12	133.5	OOM	OOM	OOM	OOM	87.0	72.2	1.53x
		16	139.9	OOM	OOM	OOM	OOM	116.6	79.8	1.2x
	4	4	126.4	142.3	OOM	OOM	117.4	41.3	33.1	0.89x
		8	150.4	138.2	OOM	OOM	148.5	66.1	60.5	1.01x
		12	167.1	OOM	OOM	OOM	163.9	84.1	75.0	1.02x
		16	175.7	OOM	OOM	OOM	164.3	102.4	93.3	1.07x
20	1	4	48.0	OOM	OOM	OOM	OOM	OOM	15.5	3.1x
		8	73.0	OOM	OOM	OOM	OOM	OOM	30.4	2.4x
		12	95.8	OOM	OOM	OOM	OOM	OOM	42.8	2.24x
		16	105.7	OOM	OOM	OOM	OOM	OOM	61.2	1.73x
	2	4	63.3	OOM	OOM	OOM	OOM	OOM	25.3	2.5x
		8	101.5	OOM	OOM	OOM	OOM	OOM	48.4	2.1x
		12	117.4	OOM	OOM	OOM	OOM	OOM	61.9	1.9x
		16	129.6	OOM	OOM	OOM	OOM	OOM	78.2	1.66x
	4	4	103.0	OOM	OOM	OOM	OOM	OOM	OOM	-
		8	139.6	OOM	OOM	OOM	OOM	OOM	OOM	-
		12	151.3	OOM	OOM	OOM	OOM	OOM	OOM	-
		16	161.7	OOM	OOM	OOM	OOM	OOM	OOM	-